Data Repository Item For:

C.A. Currie, C. Beaumont, and R.S. Huismans

The fate of subducted sediments: a case for backarc intrusion and underplating

Supplementary Information on Numerical Modelling Approach

The initial model geometry is shown in Figure DR1. The two-dimensional model domain has a width of 2000 km and depth of 660 km. The isostatically adjusted oceanic plate consists of a 2 km sediment layer, 6 km oceanic crust, and 84 km mantle lithosphere. The continental lithosphere has a 24 km upper/mid crust, 12 km lower crust, and 84 km mantle lithosphere. Both plates are underlain by sublithospheric mantle. At the boundary between the two plates, an inclined weak seed is used for subduction initiation.

GOVERNING EQUATIONS

The thermal-mechanical evolution of the system is governed by the two-dimensional conservation of mass, force balance, and energy balance equations, under the assumptions of plane strain, incompressibility, and zero Reynolds number:

$$\frac{\partial v_j}{\partial x_j} = 0 \tag{1}$$

$$\frac{\partial \sigma_{ij}}{\partial x_i} + \rho g_j = 0 \qquad i,j=1,2 \tag{2}$$

$$\rho c_p \left(\frac{\partial T_K}{\partial t} + v_i \frac{\partial T_K}{\partial x_i} \right) = k \frac{\partial}{\partial x_i} \frac{\partial T_K}{\partial x_i} + A + v_i \alpha g_i T \rho \tag{3}$$

where $x_{i,j}$ are spatial coordinates, $v_{i,j}$ are components of velocity, ρ is density, g_j is (vertical) gravitational acceleration, c_p is specific heat, T_K is absolute temperature, t is time, k is thermal conductivity, A is volumetric radioactive heat production, and α is the volumetric thermal expansion coefficient. Repeated indices imply summation. Shear heating could be included in the energy balance (Equation 3) but has been shown to lead to relatively minor increases in temperature (~50°C) (C. Warren, pers comm.) in comparable models that also involve continental collision. Both types of models involve the deformation of relatively weak material at moderate strain rates which explains the low level of the strain heating. The associated stress tensor is:

$$\sigma_{ij} = -P\delta_{ij} + \sigma'_{ij} = -P\delta_{ij} + 2\eta_{eff}\dot{\varepsilon}_{ij} \tag{4}$$

is P is pressure (mean stress), σ'_{ij} is the deviatoric stress tensor, η_{eff} is effective viscosity, δ_{ij} is the Kronecker delta (1 for i=j and 0 otherwise), and the strain rate tensor is:

$$\dot{\varepsilon}_{ij} = \frac{1}{2}\left(\frac{\partial v_i}{\partial x_j} + \frac{\partial v_j}{\partial x_i} \right) \tag{5}$$

These equations are solved using Arbitrary Lagrangian-Eulerian (ALE) finite element techniques (Fullsack, 1995). Mechanical and thermal calculations are carried out on an Eulerian mesh that stretches vertically to conform to the upper model surface. The Eulerian mesh has 200 elements in the horizontal direction (10 km width) and 126 elements vertically, with 75 elements in the upper 150 km (2 km height) and 51 elements in the lower 510 km (10 km height). Material properties are tracked on a Lagrangian mesh and additional Lagrangian tracer particles which are advected with the model velocity field.

MATERIAL PROPERTIES

All materials in the models have a viscous-plastic rheology. For a deviatoric stress below the frictional plastic yield, deformation is viscous, with an effective viscosity (η_{eff}^{v}) given by:

$$\eta_{eff}^{v} = f(B^*)\left(\dot{I}'_2\right)^{(1-n)/n} exp\left(\frac{Q + PV^*}{nRT_K} \right) \tag{6}$$

where f is a scaling factor, $\dot{I}'_2$ is the square root of the second invariant of the strain rate tensor ($\dot{I}'^{\,2}_2 = \frac{1}{2}\dot{\varepsilon}_{ij}\dot{\varepsilon}_{ij}$), R is the gas constant (8.3145 J mol^{-1} K^{-1}), and B^*, n, Q and V^* are the pre-exponential viscosity parameter, stress exponent, activation energy and activation volume from laboratory data. The parameter B^* includes a conversion from the uniaxial laboratory experiments to the plane strain state of stress used in the numerical models. The factor f allows the effective viscosity to be scaled upward or downward relative to that of laboratory-derived flow laws, to approximate variations in strength due to changes in composition or volatile content relative to laboratory samples and as a method for investigating the model sensitivity to variations in effective viscosity associated with uncertainties in the laboratory-derived parameters (Beaumont et al., 2006).

Frictional-plastic deformation is defined by a Drucker-Prager yield criterion:

$$J'_2 = c_0 + P\sin\phi_{eff} \qquad (7)$$

where J'_2 is the square root of the second invariant of the deviatoric stress tensor ($J'^{\,2}_2 = \frac{1}{2}\sigma'_{ij}\sigma'_{ij}$), c_0 is the cohesion, ϕ_{eff} is the effective internal angle of friction, which includes the effects of pore fluid pressure (e.g. Beaumont et al., 2006). Plastic deformation is modelled by defining an effective viscosity that places the state of stress on yield (Fullsack, 1995). Plastic materials strain soften through a decrease in ϕ_{eff} from 15° to 2° over accumulated strain (I'_2) of 0.5 to 1.5, as an approximation of material weakening or an increase in pore fluid pressure (reduction in ϕ_{eff}) with increasing strain.

The rheological parameters for all model materials are given in Table DR1. The viscous rheologies of the sublithospheric mantle and mantle lithospheres are based on a wet olivine rheology (Karato and Wu, 1993), with the effective viscosity of the mantle lithosphere scaled upward by a factor of 10 (f=10), to approximate strengthening due to a dehydration and melt depletion during formation. The viscous rheology of the upper continental crust is based on the Gleason and Tullis (1995) wet quartzite flow law, and viscous rheologies for the oceanic crust and lower continental crust follow the Mackwell et al. (1998) flow law for dry Maryland diabase. The model sediments have a viscous rheology based on the flow law for wet quartzite (Gleason and Tullis, 1995). Although this is termed a "wet" flow law, the samples that were analyzed were in "as received" condition, not water-saturated. Gleason and Tullis (1995) estimate that the samples contained only a small amount of water (~0.15 wt %). A comparison between this flow law and other published wet quartz flow laws shows that the Gleason and Tullis (1995) flow law is among the strongest and overlaps with the strength of some dry quartz flow laws. The sensitivity of the model results to variations in sediment strength (e.g., owing to variations in water content, composition or metamorphic phase changes) is investigated by scaling the effective viscosity relative to the reference Gleason and Tullis (1995) flow law, using the factor f.

The thermal conductivity of all materials is 2.25 W m^{-1} K^{-1} at temperatures below 1344ºC (i.e., the base of the continental lithosphere at the start of the models), with a linear increase to 52 W m^{-1} K^{-1} at 1376ºC. The enhanced conductivity at high temperature corresponds to a scaling of the thermal conductivity by the Nusselt number of upper mantle convection, and thus maintains a nearly constant heat flux to the base of the lithosphere and an adiabatic temperature gradient in the sublithospheric mantle, without the need to explicitly model convection in the upper mantle (Pysklywec and Beaumont, 2004). Radioactive heat production is 1.0, 1.15, 0.55 μW/m^3, for the sediments, upper and lower continental crust, respectively and 0 μW/m^3 elsewhere.

The thermal and mechanical fields are coupled through the temperature-dependent viscous rheology (Equation 6). In addition, all materials have a density that varies with temperature (in °C):

$$\rho(T) = \rho_0\left[1 - \alpha\left(T - T_0\right)\right] \qquad (8)$$

where ρ_0 is the reference density at temperature T_0 and the volumetric thermal expansion coefficient, α, is 3×10^{-5} K^{-1} (Table DR1). The lower continental crust and oceanic crust undergo a phase change to higher density material when these materials are at pressures and temperatures within the eclogite stability field (Hacker, 1996). The phase change affects only the density; thermal and rheological parameters are not changed. The smaller increase in the density of the lower continental crust corresponds to a density change appropriate for an intermediate composition, as opposed to the basalt-eclogite phase transition for the oceanic crust.

The model sediment is interpreted to be dominantly terrigenous with a small pelagic component (GLOSS composition of Plank and Langmuir, 1998). A reference density of 2800 kg/m^3 is used, such that sediments are 550 kg/m^3 less dense than mantle materials at 800°C, and density changes associated with phase changes during subduction are not included. This density is consistent with felsic continental crust at ultrahigh pressure (UHP) conditions (>2.6 GPa) (e.g., Walsh and Hacker, 2004, Massonne et al., 2007). The sensitivity of the model results to sediment density were tested for sediment reference densities of 2800-3300 kg/m^3, corresponding to a decrease in the sediment buoyancy from 550 to 60 kg/m^3 relative to the mantle at 800°C. This range of densities is similar to

the range of densities given by Massonne et al. (2007) for continental crust and pelagic sediments. Experimental work suggests that continentally-derived sediments only become more dense than the mantle at depths greater than ~200km (Irifune et al.,1994).

BOUNDARY CONDITIONS AND INTIAL THERMAL STRUCTURE

The mechanical boundary conditions are: 1) oceanic lithosphere is introduced through the left boundary at 5 cm/yr, 2) the continental lithosphere at the right boundary is pinned (v=0 cm/yr), 3) a small outflux velocity (Vb) along the side boundaries of the sublithospheric mantle maintains mass balance, 4) the top surface is free, and 5) the basal boundary is no-slip.

The thermal boundary conditions are: 1) constant temperature of 0ºC along the top boundary, 2) constant temperature of 1560ºC along the basal boundary, 3) prescribed geotherm for the incoming oceanic lithosphere consistent with thermal structure of an oceanic plate with an age greater than 70 Myr (Stein and Stein, 1992), and 4) no conductive heat flux along the other side boundaries. These boundary conditions and the thermal properties given above are used to calculate the initial two-dimensional steady-state thermal structure for the model domain. The laterally-averaged initial continental and oceanic geotherms are shown in Figure DR1. The continental lithosphere has an initial thermal structure similar to that of Phanerozoic continental regions (Poudjom Djomani et al., 2001), with a surface heat flow of 55 mW/m^2 and a Moho temperature (36 km depth) of 568°C. Its starting 120 km thickness is consistent with the intersection of a conductive geotherm with a 1296°C mantle adiabat.

TABLE DR1. MATERIAL PARAMETERS IN THE NUMERICAL MODELS

	Sediments	Cont. upper-mid crust	Cont. lower crust / oceanic crust	Cont. / oceanic mantle lithosphere	Sublithospheric mantle
Plastic rheology					
c_0 (MPa)	2	2	0	0	0
ϕ_{eff}	15º to 2º	15º to 2º	15º to 2º	15º to 2º	15º to 2º
Viscous rheology					
f	1	5	0.1	10	1
A (Pa^{-n} s^{-1})	1.10×10^{-28}	1.10×10^{-28}	5.05×10^{-28}	3.91×10^{-15}	3.91×10^{-15}
B^* (Pa s$^{1/n}$)*	2.92×10^{6}	2.92×10^{6}	1.91×10^{5}	1.92×10^{4}	1.92×10^{4}
N	4.0	4.0	4.7	3.0	3.0
Q (kJ mol^{-1})	223	223	485	430	430
V^* (cm^3 mol^{-1})	0	0	0	10	10
Thermal parameters					
k (W m^{-1} K^{-1})†	2.25	2.25	2.25	2.25	2.25
A (μW m^{-3})	1.00	1.15	0.55 / 0.0	0	0
c_p (J kg^{-1} K^{-1})	750	750	750	1250	1250
Density					
ρ_0 (kg m^{-3})	2800	2800	2950 / 2950	3250	3250
T_0 (ºC)	200	200	500 / 0	1344	1344
Eclogite ρ_0 (kg m^{-3})	--	--	3100 / 3300	--	--
Eclogite T_0 (ºC)	--	--	500 / 500	--	--
α (K^{-1})	3.0×10^{-5}	3.0×10^{-5}	3.0×10^{-5}	3.0×10^{-5}	3.0×10^{-5}

* $B^* = \left(2^{(1-n)/n} 3^{-(n+1)/2n}\right) A^{-1/n}$. The term in brackets converts the pre-exponential viscosity parameter from uniaxial laboratory experiments (A) to the plane strain conditions of the numerical models

† thermal conductivity at temperatures less than 1344ºC; at higher temperatures, thermal conductivity increases linearly from 2.25 W m^{-1} K^{-1} at 1344ºC to 52.0 W m^{-1} K^{-1} at 1376ºC

REFERENCES CITED

Beaumont, C., Nguyen, M., Jamieson, R., and Ellis, S., 2006, Crustal flow modes in large hot orogens, *in* Law, R.D., Searle, M.P., and Godin, L., eds., Crustal flow, ductile extrusion and exhumation in continental collision zones: Special Publication 268, Geological Society of London, p. 91-145.

Gleason, G.C., and Tullis, J., 1995, A flow law for dislocation creep of quartz aggregates determined with the molten salt cell: Tectonophysics, v. 247, p. 1-23.

Hacker, B.R., 1996, Eclogite formation and the rheology, buoyancy, seismicity, and H_2O content of oceanic crust, *in* Bebout, G.E., Scholl, D.W., Kirby, S.H., and Platt, J.P., eds., Subduction top to bottom: Geophysical Monograph 96, American Geophysical Union, p. 337-346.

Irifune, T., Ringwood, A.E., and Hibberson, W.O., 1994, Subduction of continental crust and terrigenous and pelagic sediments: an experimental study: Earth and Planetary Science Letters, b. 126, p. 351-368, doi: 10.1016/0012-821X(94)90117-1.

Karato, S., and Wu, P., 1993, Rheology of the upper mantle: A synthesis: Science, v. 260, p. 771-778.

Mackwell, S.J., Zimmerman, M.E., and Kohlstedt, D.L., 1998, High-temperature deformation of dry diabase with application to tectonics on Venus: Journal of Geophysical Research, v. 103, p. 975-984.

Massonne, H.-J., Willner, A.P., and Gerya, T., 2007, Densities of metapelitic rocks at high to ultrahigh pressure conditions: What are the geodynamic consequences?: Earth and Planetary Science Letters, v. 256, p. 12-27, doi: 10.1016/j.epsl.2007.01.013.

Plank, T., and Langmuir, C., 1998, The chemical composition of subducting sediment and its consequences for the crust and mantle: Chemical Geology, v. 145, p. 325–394, doi: 10.1016/S0009-2541(97)00150-2.

Poudjom Djomani, Y.H., O'Reilly, S.Y., Griffin, W.L., and Morgan, P., 2001, The density structure of subcontinental lithosphere through time: Earth and Planetary Science Letters, v. 184, p. 605, 621.

Pysklywec, R.N., and Beaumont, C., 2004, Intraplate tectonics: Feedback between radioactive thermal weakening and crustal deformation driven by mantle lithosphere instabilities: Earth and Planetary Science Letters, v. 221, p. 275-292.

Stein, C.A., and Stein, S., 1992, A model for the global variation in oceanic depth and heat flow with lithospheric age: Nature, v. 359, p. 123-129.

Walsh, E.O., and Hacker, B.R., 2004, The fate of subducted continental margins: Two-stage exhumation of the high-pressure to ultrahigh-pressure Western Gneiss Regions, Norway: Journal of Metamorphic Geology, v. 22, p. 671–687, doi: 10.1111/j.1525-1314.2004.00541.x.

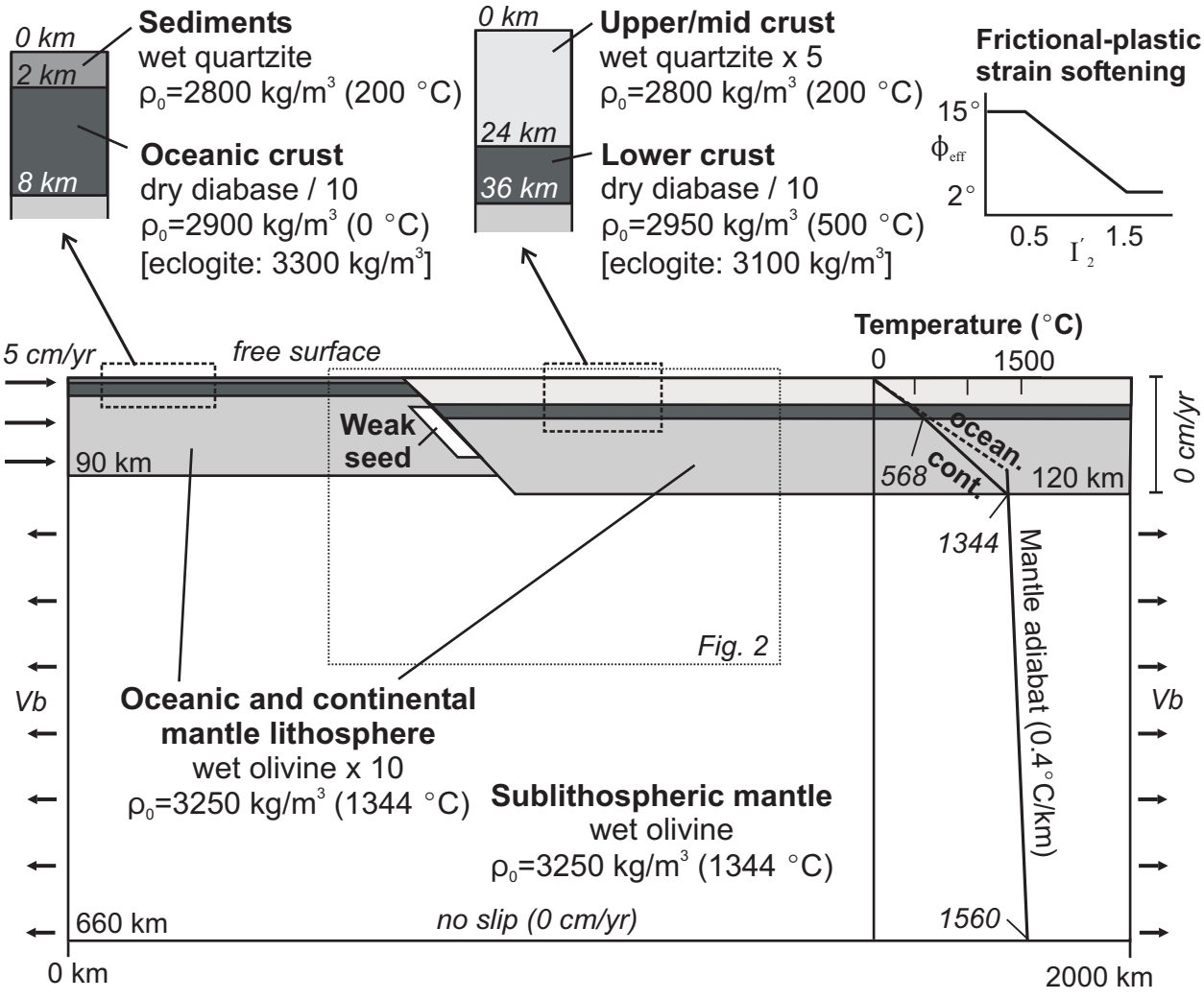

Figure DR1. Initial design of the 2D model. See text for details.